Thermochimica Acta, 168 (1990) 187–195
Elsevier Science Publishers B.V., Amsterdam

THERMAL AND SPECTRAL STUDY OF 5-CHLORO-4-β-GLYCOPYRANOSYLAMINOPYRIMIDINE DERIVATIVES

A. SÁNCHEZ, M. NOGUERAS, M^a. L. QUIJANO, M. MELGUIZO and R. LÓPEZ *

Departamentos de Química Inorgánica y Orgánica, Facultad de Ciencias Experimentales, Universidad de Granada, 23071-Jaén (Spain)

(Received 16 February 1990)

ABSTRACT

The synthesis, spectral features (^1H NMR and IR spectroscopies) and thermal characterization of seven 5-chloro-4-glycopyranosylamino-6-oxo-pyrimidine derivatives are reported. The IR spectroscopy examination allowed some aspects of the pyrolytic decomposition mechanisms of the compounds to be established.

INTRODUCTION

In view of the biological activity of many pyrimidine derivatives, their nucleosides and some of their metal complexes [1–8], we are involved in the synthesis and characterization of such compounds. Spectral and thermal studies of several series of pyrimidine nucleoside analogues have already been published [9–13], and as a continuation of these studies we now present the results obtained from seven 5-chloro-4-glycopyranosylamino pyrimidine derivatives, having the general formula shown in Scheme I (below).

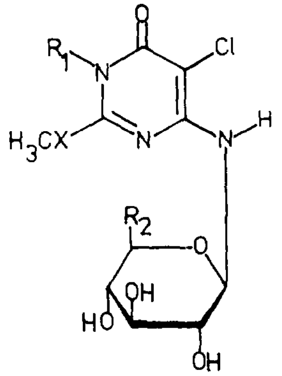

COMPOUND	X	R_1	R_2
A	O	H	CH_2OH
B	O	CH_3	H
C	O	CH_3	CH_2OH
D	S	H	H
E	S	H	CH_2OH
F	S	CH_3	H
G	S	CH_3	CH_2OH

---

* Author to whom correspondence should be addressed.

EXPERIMENTAL

The seven compounds were synthethized by a previously reported method [14]. Microanalyses for C, H and N were performed at the Instituto Nacional de Química Orgánica (CSIC, Madrid), Table 1, while their in vivo anti-cancer activities, as L-1210 inhibitors, were measured at the National Cancer Institute (Bethesda, MD) [14]. The proposed formulae, from analytical data, are collected in Table 1.

^{1}H NMR spectra were obtained with a Hitachi–Perkin–Elmer R-600 spectrophotometer, using $CDCl_3$ and DMSO-d_6 as solvents, and TMS as internal standard. IR spectra were recorded with a 4250 Beckman spectrophotometer using KBr pellets, and UV–visible spectra with a Beckman 25 spectrophotometer and aqueous solutions of the samples. DSC plots were obtained with a Mettler DSC-20 differential scanning calorimeter at a heating rate of 10 °C min^{-1}, using samples of 0.940–1.098 mg. Thermogravimetric curves were obtained with a Mettler TG 50 thermobalance in a static, pure-air atmosphere, at a heating rate of 10 °C min^{-1}, with samples of 9.573–11.180 mg.

RESULTS AND DISCUSSION

Spectral study

The most significant IR spectral bands of the compounds are detailed in Table 2. As expected, the $\nu(OH)_{sugar}$ and $\nu(N-H)$ bands are observed at high frequency, although the latter are hidden by the former, which are broadened. In some cases (compounds A, B, C and F) very sharp $\nu(OH)$ bands appear in the IR spectra when water of hydration is present. These sharp $\nu(OH)$ bands are superimposed on the $\nu(OH)_{sugar}$ bands, but they

TABLE 1

Yields and analytical data of the compounds (the values calculated from the proposed formulae are in parentheses)

Compound	Yield (%)	Analytical data			Formula
		C	H	N	
A	72	35.50(35.35)	5.29(5.39)	11.21(11.24)	$C_{11}H_{16}N_3O_7Cl \cdot H_2O$
B	93	38.82(38.89)	5.33(5.34)	12.20(12.37)	$C_{11}H_{16}N_3O_6Cl \cdot H_2O$
C	80	38.69(38.98)	5.40(5.45)	11.28(11.37)	$C_{12}H_{18}N_3O_7Cl \cdot H_2O$
D	91	37.05(37.10)	4.29(4.36)	12.90(12.98)	$C_{10}H_{14}N_3O_5SCl$
E	87	33.92(33.89)	5.21(5.17)	10.70(10.78)	$C_{11}H_{16}N_3O_6SCl \cdot 2H_2O$
F	90	38.01(38.09)	5.11(4.94)	12.10(12.12)	$C_{11}H_{16}N_3O_5SCl \cdot 0.5H_2O$
G	92	39.01(39.19)	5.16(4.93)	11.12(11.42)	$C_{12}H_{18}N_3O_6SCl$

TABLE 2

IR spectral data (ν in cm^{-1})

Compound	ν(OH)	ν(NH)	ν(C–H)	ν(C=O)	ν(C=C) + ν(C=N)	ν(C–O) + ν(C–N)
A	3360 s,b	3150 b	2869 w 2910 w	1675 s	1595 s 1610 s	1010 m 1030 m 1040 m 1080 m 1110 m
B	3400–3340 s	3240 b	2930 w 2860 w	1665 s	1615 s 1540 s	1000 w 1040 w 1050 m 1065 m 1080 w 1110 m
C	3460–3360 s	3250 b	2840 w 2855 w 2960 w	1660 s	1630 s 1550 s	1010 w 1030 w 1040 w 1080 w 1100 w
D	3380 vb		2830–3000 w	1660 s	1600 s 1510 s	1005 w 1025 w 1040 s 1060 m 1085 m 1100 w
E	3400 vb		2850–3000 w	1655 s	1550 s	1000 w 1040 m 1060 m 1085 m 1105 w
F	3400 vb	3400 vb	2930 w 2860 w	1675 s	1610 s 1530 s	1000 w 1020 w 1045 m 1055 m 1070 m 1090 w 1100 w
G	3440 vb 3380 vb	3270 s	2940 w 2910 w 2880 w	1640 s	1605 s 1530 s	1010 w 1020 w 1035 m 1045 m 1070 w 1110 w

vb, very broad; b, broad; s, strong; m, medium; w, weak.

disappear when, the samples are heated up to the final dehydration temperature.

The ν(C=O) frequencies are lower than those of the corresponding acetylated sugar homologues [13], suggesting higher aromaticity of the present compounds. On the other hand, ν(C=O) values are higher (indicating lower aromaticity) than those of the corresponding unchlorinated homologues [11], owing to the electron-attracting character of the Cl atom at C-5. The remaining assigned bands in Table 2 are similar to those present in the IR spectra of the homologous unchlorinated derivatives [11].

The assignment of the ^1H NMR spectra has already been reported [14]. The range of δ values corresponding to C_4–NH groups (7.00–7.10 ppm) is similar to that in 5-chloro derivatives in which the sugar residues are acetylated, suggesting the absence of any hydrogen-bridge interaction affecting the NH group [13,15].

Thermal study

TG and DSC plots of the seven compounds studied appear in Figs. 1 and 2, respectively. From these figures the thermal data appearing in Table 3 were obtained. Three classes of processes were identified from Figs. 1 and 2, namely: desolvation, melting and pyrolytic decomposition.

Desolvation processes are in accordance with the proposed formulae for the seven compounds, except in the case of compound G in which a negligible amount of water is present (see composition data). The high dehydration energies point to a high degree of hydrogen bridge interaction between the water molecules and the compounds. This is a general feature of

TABLE 3

TG and DSC data

Compound	Dehydration		Fusion		Start of the pyrolysis	Pyrolysis	
	T (°C) (endo)	ΔH (kJ mol^{-1})	T(°C) (endo)	ΔH (kJ mol^{-1})	T (°C)	T (°C)	ΔH (kJ mol^{-1})
$A \cdot H_2O$	100.9	−80.79	180.2 [a]	−12.34 [a]	185	exo 243.0	83.90
$B \cdot H_2O$	152.4	−57.46	241.9	−58.05	190	exo 250.5	89.28
$C \cdot H_2O$	118.2	−27.32			170–180	exo 245.2	112.01
D			234.4	−62.22	235	exo 237.1	49.98
$E \cdot 2H_2O$	94.1	−52.77	199.8 [a]	−46.69 [a]	200	exo [c] 203.4	– [c]
$F \cdot 1/2H_2O$	94.6	−28.16	240.2 [a]	−59.57	240	exo [c] 241.5	43.12
$G \cdot H_2O$	83.2	−7.85	201.8 [a]	−66.96	204	exo [c] 203.8	– [c]

[a] The endothermic overlaps with the start of decomposition.

[b] Corresponds to a 2% water humidity.

[c] Overlaps with the endotherm of the fusion.

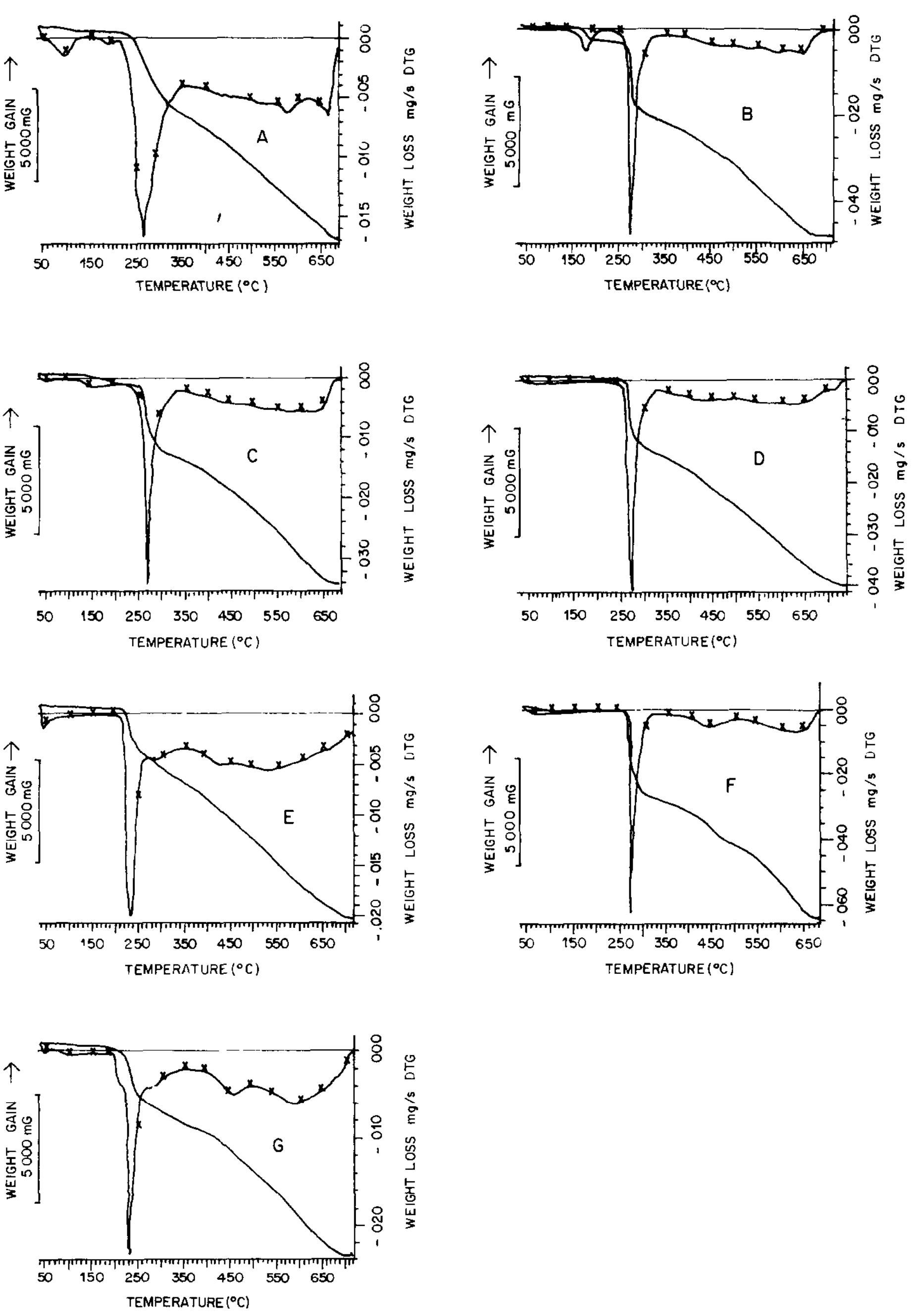

Fig. 1. TG curves.

all 4-glycopyranosylaminopyrimidine derivatives studied so far, suggesting that it is the glycoside residue which is involved in such interactions.

On the other hand, in all DSC plots a sharp endothermic effect is present

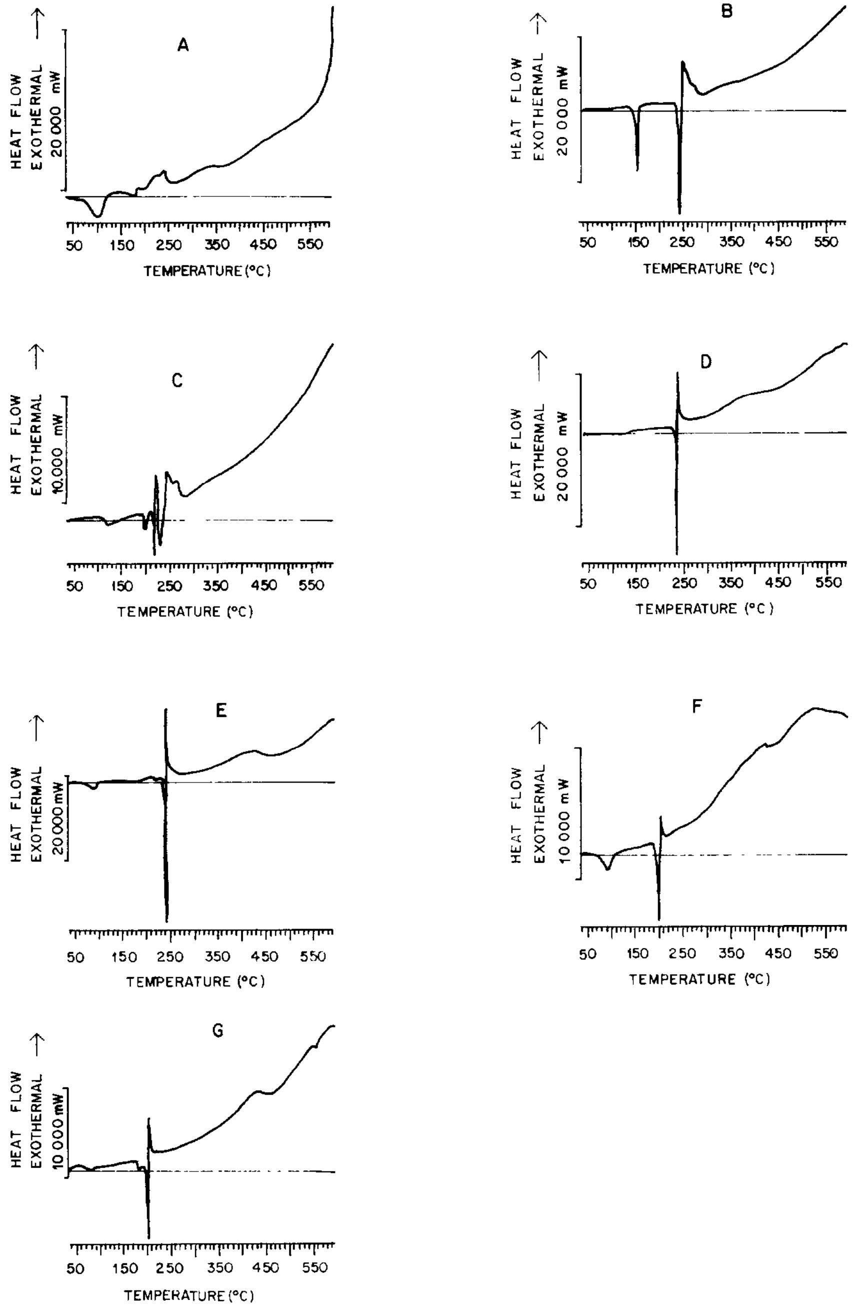

Fig. 2. DSC curves.

which can be assigned to melting processes (no weight losses were detected in the corresponding TG plots in the temperature ranges at which those endothermic processes take place). In the cases of compounds A, C and E, in which more than one endothermic event is present, the accurate assignment of the one which corresponds to melting was made by observing the fusion processes in a melting apparatus. The energies of those fusion processes are high, indicating strong intermolecular interactions. This behaviour is similar to that in other series of 4-glycopyranosylamino-6-oxo-pyrimidine derivatives with H or Cl attached to C-5, all of which melt [9,11,13], but contrasts with that of similar derivatives with, e.g. –NO substituents on C-5, which do not melt. This demonstrates the role of the C-5 substituent in strong intermolecular interaction, resulting, possibly, in the formation of polymers.

The pyrolytic decomposition of compounds A, B, and C starts immediately after the corresponding dehydration, as can be seen in the TG and DSC diagrams. In fact, the weight loss effects in the TG curves overlap in these compounds, with gradual weight losses corresponding to the onset of pyrolytic decomposition. In the case of compound A the calculated overall weight loss, up to the start of the first abrupt weight loss, is in accordance with the theoretical value (corresponding to the loss of water of hydration and the OCH_3 substituent on C-2) so the small exothermic effect appearing in the DSC diagram after melting could correspond to the combustion of the OCH_3 group mentioned. Nevertheless, no noticeable change occurred in the IR spectrum of compound A when heated up to the final temperature of this exotherm (no doubt due to the presence of the C–H and C–O bands of the sugar residue).

In the case of compound C, two endothermic effects and a weak, but sharp, one at 200–225 °C, all of which precede melting, take place during the onset of pyrolytic decomposition. These can be assigned to the loss and subsequent combustion of substituents (including probably an OCH_3 group) on the pyrimidine ring. This was proved by the fact that all the characteristic bands of such a ring, as well as those of the glycoside residue and the $C_6{=}O$ group were clearly observed in the IR spectrum of a sample of compound B heated up to the melting temperature. It is interesting to observe that the compounds with OCH_3 substituted on C-2 decompose at lower temperatures than the SCH_3 analogues (see Table 3), provided that an electron-attracting group exists on C-5 (e.g. NO or Cl group) [9–13]. This can be explained in terms of reduced electron density of the pyrimidine ring, promoted by the C_5–NO electron-attractive substituent, labilizing the C_5–OCH_3 bond because of the high electronegativity of the oxygen atom. On the contrary, when the substituents on C-5 are not electron-attracting, then the temperatures found for the onset of pyrolytic decompositions are similar for both C_2–OCH_3 and C_2–SCH_3 derivatives [9,11].

All the compounds suffer a first abrupt weight loss between 230 °C and 250 °C (see TG diagram in Fig. 1). In the case of compounds D, E, F and G these correspond to the onset of pyrolytic decomposition and are accompanied by an exothermic effect, as can be seen in all seven DSC diagrams. Nevertheless, in almost all cases the exotherm overlaps with the endotherm corresponding to melting of the samples, so the energies of both melting and of the exotherm accompanying the abrupt weight loss must be viewed as approximate only.

The similarity between the TG curves suggests a similarity in the thermal decomposition corresponding to this first step. To confirm this, samples of the seven compounds were heated up to the final temperature of the abrupt weight loss and their IR spectra in the high frequency range recorded (4000–600 cm^{-1}). All the spectra show clearly the almost total loss of ν(OH) and of bands corresponding to ν(C–O) stretching vibrations of the sugar residues. On the other hand, the ν(C–H) bands (due to the $-CH_3$ groups and to the C–H bands of the sugar residue) do not disappear completely. Moreover, the weight losses found in the TG curves (at the final temperatures) are significantly lower than the theoretical values corresponding to the sugar residues. From all these data, it can be inferred that the combustion of the sugar residue is the initial stage in the pyrolytic decomposition of compounds D, E, F and G. In the case of compounds A, B and C, the pyrolytic decomposition starts with the loss, and combustion, of the $-OCH_3$ substituents on C-2 and goes on uninterrupted by combustion of the sugar residue. The final temperature of this step could not be established because of the absence of intermediate stable species.

ACKNOWLEDGEMENTS

The anti-carcinogenic activity data are the results of screening performed under the auspices of the Developmental Therapeutics Program, Division of Cancer Treatment, NCI Bethesda, MD.

The authors thank the Consejeria de Educación, Junta de Andalucía, for the award of a fellowship of the Plan de Formación del Personal Investigador to two of them (M.L. Quijano and M. Melguizo). This work was supported by research grants from the CICYT (No. 89/414).

REFERENCES

1 J.L. Rideout, D.W. Henry and L.M. Beachan III (Eds.), Nucleosides, Nucleotides and their Biological Application, Academic Press, New York, 1983.
2 T.K. Bradshaw and B. Hutchinson, Chem. Soc. Rev., 6 (1977) 43.
3 P.F. Torrence, Anticancer and Interferon Agents. Synthesis and Properties, Vol. 24, Dekker, New York, 1984.
4 J. Reedijk, Pure Appl. Chem., 59 (1987) 181.
5 S.M. Skinner, J.M. Swatzell and R.W. Lewis, Res. Commun. Chem. Pathol. Pharmacol., 19 (1978) 165.
6 M. Das and S.E. Livingstone, Br. J. Cancer, 38 (1978) 325.
7 S. Kirschner, Y.K. Wei, D. Francis and J.G. Bergman, J. Med. Chem. Pathol. Pharmacol., 27 (1978) 165.

8 E. Dubler and E. Gyr, Inorg. Chem., 27 (1988) 1466.
9 R. López Garzón, A. Sánchez Rodrigo, M. Nogueras Montiel and J. Negrillo Pérez, Thermochim. Acta, 96 (1985) 59.
10 A. Sánchez Rodrigo, M. Nogueras Montiel, R. López Garzón, M. Gutierrez Valero and E. Colacio Rodriguez, Thermochim. Acta, 86 (1985) 199.
11 R. López Garzón, M. Nogueras Montiel, A. Sánchez Rodrigo and J. Negrillo Pérez, Thermochim. Acta, 91 (1988) 173.
12 M. Nogueras, R. López, M. Gutierrez and A. Sánchez, J. Therm. Anal., 34 (1988) 1335.
13 R. López, M.D. Gutierrez, M.L. Quijano, M. Melguizo, M. Nogueras and A. Sánchez, Thermochim. Acta, 153 (1989) 113.
14 J. Negrillo, A. Sánchez, M. Nogueras and M. Melgarejo, An. Quím., 84C (1988) 165.
15 R. López, M. Gutierrez, M. Nogueras, A. Sánchez and C. Valenzuela, Monatsch. Chem., 117 (1986) 905.